Hindawi
International Transactions on Electrical Energy Systems
Volume 2024, Article ID 5525066, 19 pages
https://doi.org/10.1155/2024/5525066

Research Article

Optimizing MPPT Control for Enhanced Efficiency in Sustainable Photovoltaic Microgrids: A DSO-Based Approach

Debabrata Mazumdar,[1] **Pabitra Kumar Biswas**,[1] **Chiranjit Sain**,[2] **Furkan Ahmad**,[3] **Rishiraj Sarker**,[4] **and Taha Selim Ustun**[5]

[1]*Department of Electrical and Electronics Engineering, NIT Mizoram, Aizawl, Mizoram 796012, India*
[2]*Department of Electrical Engineering, Ghani Khan Choudhury Institute of Engineering and Technology, Malda, WB, India*
[3]*Division of Sustainable Development, College of Science and Engineering, Hamad Bin Khalifa University, Qatar Foundation, Doha, Qatar*
[4]*Department of Electrical and Computer Engineering, Florida International University, Miami, FL 33174, USA*
[5]*Fukushima Renewable Energy Institute, AIST (FREA), National Institute of Advanced Industrial Science and Technology (AIST), Fukushima, Koriyama 9630298, Japan*

Correspondence should be addressed to Furkan Ahmad; fuahmad@hbku.edu.qa

Received 27 December 2023; Revised 10 March 2024; Accepted 18 March 2024; Published 17 April 2024

Academic Editor: Marcos Tostado-Véliz

 The publication of this article was funded by Qatar National Library.

The output of photovoltaic (PV) systems is significantly impacted by the vagaries of ambient temperature, solar irradiance, and environmental fluctuations. To achieve the utmost attainable power from PV systems, it is desired to be efficient at the maximum power point in diverse weather climates. Maximum power point tracking (MPPT) is used to schedule a designated location from where the highest power can be harvested. In the context of solar photovoltaic systems connected with DC microgrid platforms, this study introduces a recently developed drone squadron optimization (DSO) scheme that tracks the global maximum power point under PSCS difficulties. Furthermore, an exhaustive comparative analysis has been presented among particle swarm optimization (PSO), cuckoo search algorithm (CUSA), and grey wolf optimization (GWO) under different operating environments to endorse the supremacy of the nominated technique. The suggested method performs noticeably faster than many other methods currently in use, and in addition to offering the highest power, it can also use bidirectional power flow regulation in both constant and variable air conditions. Lastly, an MPPT system interfaced with the DC microgrid based on DSO ensures a sustainable and reliable architecture to provide at load in low power generating situations.

1. Introduction

Inherent increase in energy stipulation and excess consumption of conventional resources has motivated mankind's attention toward unending power generation in the last couple of years [1, 2]. Government has increased endowment and instigated tariff-free plans to attract civilization toward environmentally hazard-free power generation [3]. Out of the numerous appearances of green energies, hot cake to the researchers is solar energy for its eminent features and opulence availability. Solar energy is well known for its spectacular applications in various large as well as small industries [4]. The PV structure is emphasized to transform absorbed photon energy accumulated from the sun and convert it into electrical energy. Here, scientists faced utmost difficulties in using PV systems because of their nonlinear electrical behaviours. As a result, finest performance is affected under rapid changes in atmospheric temperature and irradiance [5]. Considerable outcome from solar PV panel is greatly contingent on rapid changes in atmosphere and partial shading conditions (PSCS). To step up the output power in changeable atmospheric conditions, whole arrangement is assimilated with maximum power tracking (MPPT) controllers. In addition, with DC-DC converters,

these controllers vigorously run for maximum power point. Power-voltage (P-V) behaviour is trickier as multiple peaks are observed named local maximum power point (LMPP), but only the highest peak is considered in this regard named global maximum power point (GMPP) [6]. So, searching for GMPP is a crucial task to harvest maximum power and supreme performance of PV modules. Fundamental block diagram of a complete PV system has been introduced in Figure 1 which incorporates sensors for voltage as well as current measurement with a DC-DC boost converter, using various MPPT methods which control the duty cycle of converters [7].

The voltage vs. power (V-P) and voltage vs. current (V-I) plots in photovoltaic cells are nonlinear due to specific changing atmospheric conditions. Many MPPT methods have been requested by researchers in the past few years. Traditional methods (TMPPT) and soft computing methods (SC-MPPT) are the two standard approaches used to arrive at MPP. Elgendy et al. discussed the perturb and observe (P&O)-based technique to extract maximum power from standalone PV pumping system. The impact of algorithm parameters on system behaviour is examined, and the benefits and downsides of each method are noted for specific meteorological scenarios. But they fail to distinguish between local and global maximum points [7]. In order to increase the generated PV electrical energy, Lasheen et al. suggested a technique that incorporates the advantages of the ANFIS and HC techniques while mitigating their drawbacks. To evaluate the duty ratio (control signal) being applied to a boost converter for MPP tracking, a two-stage approach is suggested. However, they failed to stabilize the power in a lower settling time [8]. Sagonda et al. in their paper evaluated and contrasted the perturb and observe (P&O), increment conductance method (IC), and fuzzy logic approaches for tracking a solar PV system's maximum power point. It has been demonstrated by the authors that compared to traditional methods, the fuzzy control methodology performs better and more consistently. It had the ability to minimise power oscillations around the maximum power point (MPP) and track it more quickly [9]. Implementation of the neural network in the solar MPPT technique had been well described in [10]. The proposed paper showed good efficiency under both dynamic and static conditions. Ram et al. proposed a new flower pollination algorithm (FPA) that can attain a worldwide peak in their article [11]. An essential component of the FPA method's success in the MPPT application was its optimization procedure, which did both local and global search in a single step. Three different shade patterns are used to assess the algorithm's ruggedness: zero, mild, and strong. Regretfully, this process is very complicated compared with other traditional methods like fuzzy logic or Hill climbing methods. The primary benefits of the suggested algorithm in [12] are its ability to track GMPP and react to load variations more quickly; its use of a single-ended primary-inductor converter allows the optimization algorithm to find the GMPP over a wider operating region; and its ease of tuning due to the reduced number of parameters that need to be set. Pillai et al. introduce an effective hybrid tracking system that, by precisely identifying instances of shade, offers a suitable compromise between traditional P&O and sophisticated soft computing methods. For this, the distinctiveness of P&O's operating point conductance at the P-V curve's leftmost power peak is used. Consequently, tracking MPP in uniform irradiance and PSCS detection are the two main uses of P&O in their proposed convention [13]. Partial shading implementation of maximum power point tracking (MPPT) using cuckoo search is shown in [14]. This paper's research focuses on the 6×4 TCT configuration of PV arrays to maximise energy output regardless of the surrounding conditions. The cuckoo search method is used in this situation while taking into account shadowing scenarios. System models are created and evaluated in the MATLAB/SIMULINK environment. A real-time adaptive perturb and observe (PO) maximum power point tracking (MPPT) technique based on variable perturbation size and gain scheduled proportional (PR-P) controllers is introduced in [15]. The constant perturbation size used in the standard PO MPPT approach causes poor transient response and large continuous steady-state oscillations. These issues were addressed by the proposed control strategy by Yanarates et al. Incremental conductance (INCE) [16] comes under traditional techniques, and they proved their effectiveness under uniform irradiance situations, but the main drawback of these methods is that they are unable to create difference among various local peaks and the global peak, especially under nonuniform irradiance conditions in the P-V curve cause in most cases they stick in local peak [17]. For this, conventional techniques are not acceptable to deal with PSCS in solar PV systems.

During the past decade, a variety of soft computing-based optimization techniques, such as the neural network (NNK) and fuzzy logic controller (FLCR), have been adopted in order to overcome the limitations of conventional methods [18, 19]. However, because of their close relationship to hardware configuration and longer processing times, today's GMPP tracking primarily relies on various bio-inspired metaheuristic algorithms. Various swarm algorithms like particle swarm optimization (PSO) [20, 21], genetic algorithm (GA) [22], grey wolf optimization (GWO) [23, 24], ant colony optimization (ACO) [25], artificial bee colony (ABC) [26], slap swarm optimization (SSO) [27, 28], grasshopper optimization [29], and jelly fish optimizer [30] had been applied by the researchers to find GMPP. In the modern era, researchers observed excellent efficiency, accuracy, and low settling time in bioinspired-based optimization techniques to track GMPP [31, 32]. Bioinspired-dependent MPPT techniques are advantageous for their simplicity and accurate tracking capability in lower settling time. However, swarm-based methods create their impact in terms of more expeditious tracking. Truly speaking, every single algorithm has some own adept disadvantages for a particular business. That is why, hunting for a new scheme is always decisive for future progress in the invention path.

Here, the concerned paper pays attention to the consent of recently self-adaptive metaheuristic algorithm named the drone squadron optimization-based MPPT technique. One

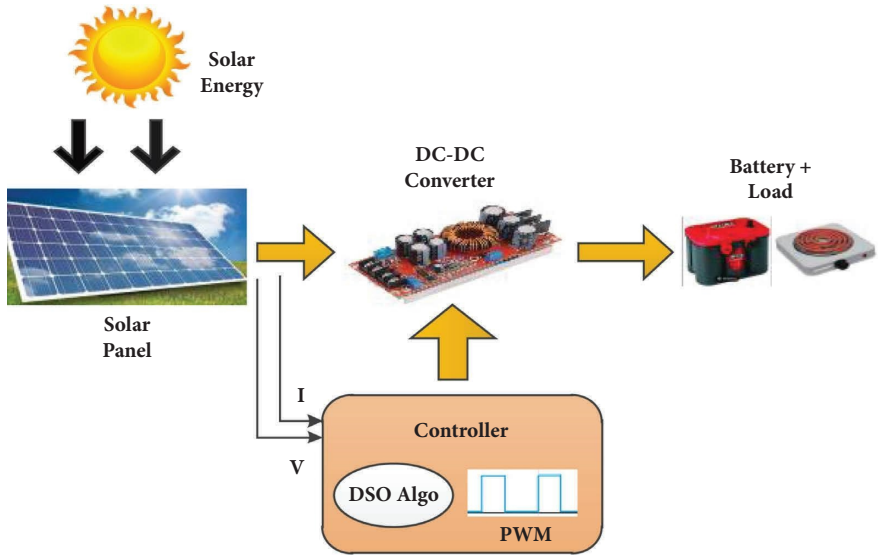

Figure 1: Fundamental schematic outline of the whole photovoltaic system.

important aspect of self-adaptive is code generation and modification along with parameter modification by its own. So, this method has the ability to change the steps that drones generally used to generate resolution. For more upgradation in MPPT performance, self-adaption is always one of the favourite choices [33]. Nowadays, most methods use man evolve adaption techniques and those are unsuitable under dynamic conditions. So, the technique that can learn on its own has a significant price. This article provides a comprehensive overview of the DSO method's operation and application in the field of solar MPPT. Moreover, a simulation with varying weather conditions was run to prove its superiority. When compared to another algorithm, the simulation result indicates that this one has the most accurate MPP tracking with PV and load power enhancement. The discussion that followed focused on the relative performance of DSO with GWO and the cuckoo search algorithm (CUSA) [34]. The design of boost converter permits nonerupted current flow from input side. Here, in Figure 2, pictorial representation of boost converter has been shown. Due to the LC filter, output side felicitates with constant smooth current waveform. The boost converter generates very less output voltage oscillation due to the presence of the first-order low pass filter. So, comprehensive impression of boost converter utilization is intrinsically lesser noise with better effectiveness of the entire system.

Exploration of this paper is accomplished in the context of DSO implementation in the MPPT field. Interpretation of the chosen approach examines under varying weather conditions and contrasted with the other procedures. The original contributions of this article are summarized as follows:

(i) A unique self-adaptive metaheuristic approach is developed which optimizes power generation on-the-fly and acts like metamorphic algorithm. Its superior fast tracking and lower oscillation features are confirmed with results obtained from different simulation cases.

(ii) Under this proposed approach, the DSO particles are capable of enduring immobilization and the oscillation becomes almost zero when one ends, and the adaptability of power convergence is almost 99.5%. The absence of these attributes in CUSA and GWO etc. results in the mislaying power and irrelevant oscillations.

(iii) A maiden attempt has been taken to introduce the self-adaptive algorithm-based MPPT method integrated with the DC microgrid platform which is examined under various irradiance conditions. It has been investigated that DSO has the capability to draw utmost power in partial shedding and invariable irradiance condition. Besides, this tracking of MPP under various irradiance scenarios, which claimed this MPPT method, is better with respect to more power harvesting, sustainability, reliability, and lower settling time in differentiation with existing MPPT structures available in the compositions.

The rest of this article is organized as follows: Section 2 provides a detailed description of the structure and modelling of photovoltaic systems, including the impact of changes in solar irradiance on their performance, with the help of current-voltage and power-voltage graph depictions.

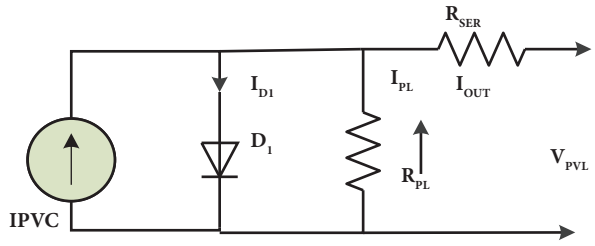

Figure 2: Analogous schematic circuit diagram of the PV cell.

In Section 3, the effects of PSCS on the execution of PV systems are discussed. Section 4 presents the drone squadron algorithm, while Section 5 outlines the development of a DSO-based MPPT. Section 6 discusses simulation and investigation results, followed by a conclusion in Section 8.

2. Design of Solar PV Module

Photovoltaic cell is an essential component of the system, though PV cell energy accumulated from the sun changes into electrical energy through photovoltaic reaction. Photon energy from daylight irradiance on photovoltaic module exceeds the energy gap, and the emanation of electrons from photovoltaic array encourages the growth of electrons to start an electric flow. The schematic circuit of a solar photovoltaic cell is shown in Figure 2 In the whole network, a current source, diode, and a set of resistors are hitched in series and parallel. PV cell output current may be intended as (1).

$$I_{\mathrm{OUT}} = I_{\mathrm{PVC}} - I_{D1} - I_{\mathrm{PL}}, \tag{1}$$

where I_{OUT}, V_{PVL} are output current and voltage from photo voltaic cell discretely. I_{PL}, I_{D1} (equation (2)), I_{PVC} are parallel resistance (R_{PL}), diode and photovoltaic current, respectively. Series resistance is noted as R_{SER}.

$$I_{D1} = I_{\mathrm{RSC}} + e^{qV_{\mathrm{PVL}+}I_{\mathrm{OUT}*}R_{\mathrm{SER}}/n\mathrm{KT}-1}, \tag{2}$$

where I_{RSC} is the reverse saturation current. q, T, n, K signifies electron charge, atmospheric temperature, and diode factor Boltzmann constant separately. The current generated in the PV cell is expressed as (3).

$$I_{\mathrm{PVC}} = \frac{W}{W_0}\left(I_{\mathrm{SCN}} + \lambda\left(T - T_0\right)\right). \tag{3}$$

Short circuit current is designated by $I_{\mathrm{SCN}}, T_{0,}$ and W_0 are temperature and reference irradiance separately. λ and W were noted as atmospheric temperature and irradiance coefficient. (4) represents the I_{OUT} after combining (2) and (3).

$$I_{\mathrm{OUT}} = I_{\mathrm{PVC}} - I_{\mathrm{RSC}} + \left[e^{q\frac{V_{\mathrm{PVL}+}I_{\mathrm{OUT}*}R_{\mathrm{SER}}}{n\mathrm{KT}}} - 1\right] - \frac{V_{\mathrm{PVL}} + I_{\mathrm{OUT}} * R_{\mathrm{SER}}}{R_{\mathrm{PL}}}. \tag{4}$$

Production of power from separate solar cell is approx in range of 1–1.5 W which is very low. To meet the power demand, solar cells are assimilated either in series or in parallel. MPP also changes with varying atmospheric conditions. So, it is necessary to employ a controller to meet the photovoltaic load in a suitable way so that it may reach MPP.

As noticed in Figure 3 where power is intact as a function of voltage, MPP graphs are true. The corresponding equation is formulated in (5).

$$\frac{dP}{dV_{\mathrm{PVL}}} = \left\{ \begin{array}{c} 0 \text{ at MPP} \\ > 0, \quad \text{at left hand portion of MPP} \\ < 0, \quad \text{at right hand portion of MPP} \end{array} \right\}. \tag{5}$$

3. Consequence of Partial Shedding

PV system is unable to generate a uniform output when a certain portion of PV module gets variable irradiance that creates disparity with other portions of the module. As a result, partial shading condition occurs and various irradiance levels are received by the PV module [35]. Due to clouds, birds, portion of trees, and dust particles, some cells of photovoltaic array get blocked. As an outcome of this, the shaded portion of the module receives lesser solar insolation compared with uncovered parts of the module during PSCS condition. Naturally covered parts are not able to harvest desire output voltage; consequently, efficiency is hampered at that instant. By introducing bypass diode, the mismatching effect can be reduced. Bypass diodes make another way for the excessive current produced by uncovered cells. So, shaded cells are able to avoid the effect of hotspots [36]. Figure 4 appears with a shaded photovoltaic module in an array. Almost every diode gets uniform solar irradiance, i.e., 1000 W/m^2 under uniform irradiance condition, so no voltage drop will take place. Under PSCS conditions, various irradiance levels must be met by the PV module. When PV cells get various irradiance levels, various crests are observed in the power-voltage curve, but the peak related to highest power can be considered as GMPP whether others peaks are called as LMPP [37] . As numerous local crests exist in the power-voltage curve, an appropriate MPPT technique with intrinsic capability to track MPP under varying atmospheric conditions must be incorporated. This is worthwhile to say that the efficiency of the espoused MPPT method influences the overall effectiveness of the photovoltaic module [38]. Keeping these matters in mind, a unique DSO is suggested to implement an MPPT controller which has inherent ability to track GMPP within minimum settling time.

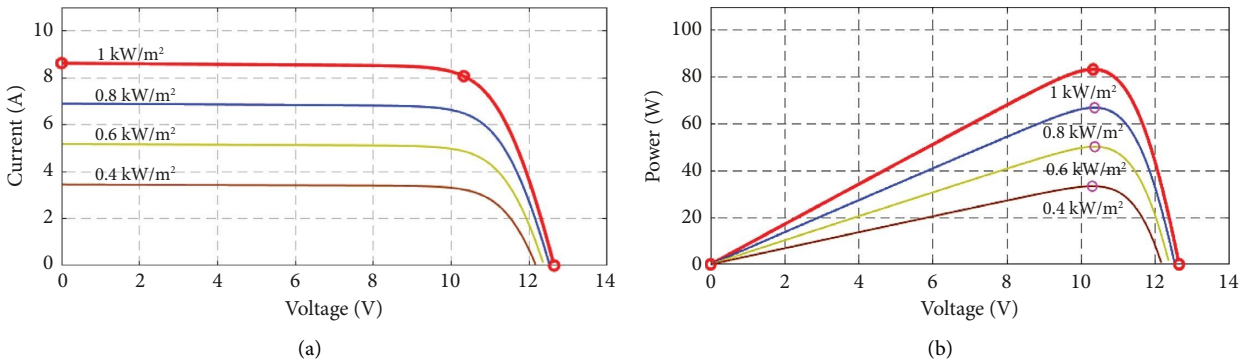

Figure 3: (a) Current vs. voltage and (b) power vs. voltage characteristics of the predefined solar cell.

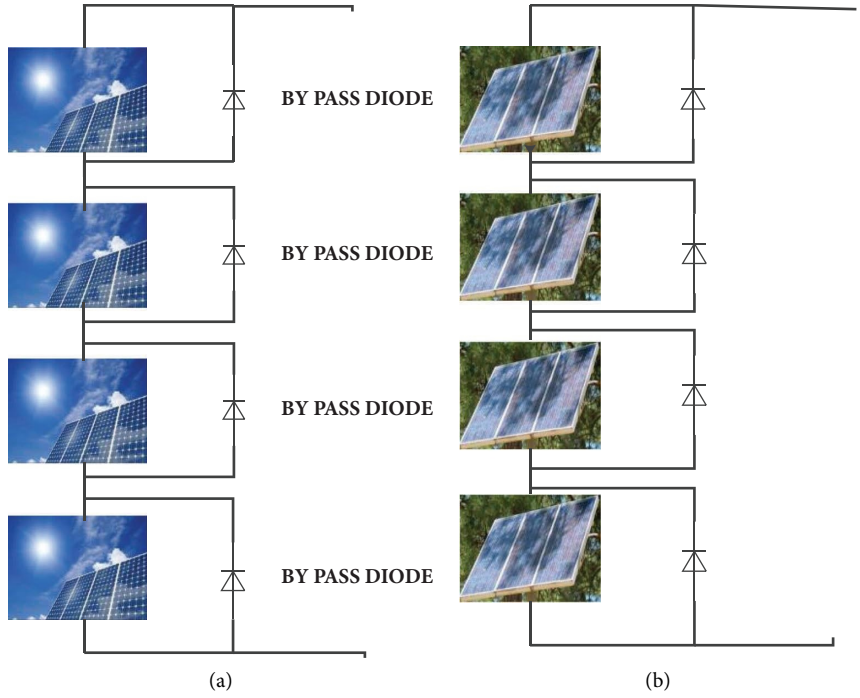

Figure 4: Solar PV cells in (a) invariable irradiance and (b) partial shading states.

4. Drone Squadron Optimization

A novel feature of like submarines or any other flying machines like helicopters and aeroplanes are able to traverse independently. With the help of sensors, they can establish communication from wide distance, even they are able to utilize solar power also. But the supreme character is that they can upgrade or improve not only their hardware but also the concerning software. Scientists simply want to utilize their upgradation ability as simple software update.

The DSO algorithm expressed in this article is possessed with several teams with a command center [39, 40]. The data which are accumulated by drones used by the command center to execute two operations: (1) to control some portion of search and (2) to configure another firmware for controlling drones as described in Figure 5. Normally, a command center is a middle place from where controlling action can be performed over drones. It collects inputs, processes the data, and executes the outputs. The command center has the ability to renovate firm were of drones whenever it concludes.

In practice, one can notice that drones have a hunt assignment (objective function) to discover a predetermined target in landscape. Values of this operation are stored in drone's sensors. It is not needed for the teams for finding a definite and distant area of landscape. In truth, all proceed from predetermined origin points that may be invariable for few teams [41]. Due to the fact that the squads have distinct firmware, they may reach distinct coordinates but may overlap in the area of exploration. In addition, one squad may restrict to go along with other squad until the command centre cryptic such character in firmware.

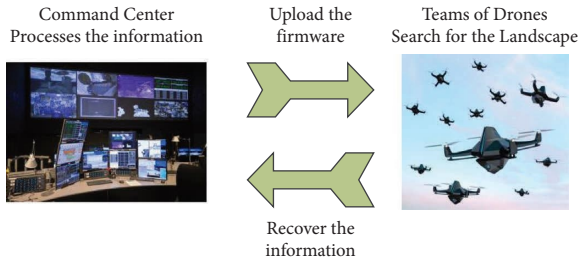

Figure 5: An abstraction of the peak DSO showing the two main modules of the system: the command center and drone teams.

As DSO has plenty of components to share with the command centre, teams, and firmware adaption, so one can think that this algorithm is more complicated rather than conventional nature-inspired algorithms. Here, a detailed algorithm is going to elaborate in lieu of simple one that might be helpful for future research [39].

4.1. Command Centre. "Heart" of the DSO algorithm is nothing, but its command centre as this is responsible for generating and commanding orders and drones accomplish the orders and return the results. The command centres upgrade the farm wears to modify the teams with the knowledge acquired by drones. Command centres employ a hyperheuristic idea to produce firmware codes. Drones utilize updated firmware along with every single piece of information allotted by the command centre to control their character. The command centre was possibly furnished with processes to learn from the search to produce superior firmware.

4.2. The Firmware. For the present drone squadron optimization edition, the firmware carrying different techniques to produce updated trial coordinates (TCOD) by perturbation; so, in the drone's firmware perturbation method, it may be treated like Heart. An upgraded firmware is created depending on the popular perturbation methods of a biased haphazard walk:

$$\mathrm{M} = \text{Departure} + \text{Offset}\ (), \tag{6}$$

$$\mathrm{TCOD} = \text{Compute}\ (\mathrm{M}). \tag{7}$$

It is necessary to compute the total perturbation formula to return the coordinates of the trial as departure is a function that recurs the authentic perturbation gesture (an absolute value). *M* represents the total perturbation formula.

A new set of departure coordinates is generated along with the offset producing function. Identifiable teams have well-defined methods of selecting departure coordinates and the process for determining offsets. The following example illustrates two perturbations for teams 1 and 2, where *K*1 represents a user-defined constant, *L* (0, 1) represents a scalar sampled from a Gaussian distribution with a zero mean and unit standard deviation, and *U* (0, 1) A represents an array of A numbers sampled from a uniform distribution where nominal value is 0, but the highest value is 1.

$$\begin{aligned} \mathrm{M}_1&: \overline{\mathrm{GBCS}} + \mathrm{K}_1 * (\overline{\mathrm{GBCS}} - \overline{\mathrm{CBCS}}\ \text{drone}),\\ \mathrm{M}_2&: \overline{\mathrm{CBCS}}\ \text{drone} + \left(\mathrm{L}(0,1) * \left(\sqrt{U(0,1)_A} + \overline{\mathrm{CBCS}}\ \text{drone}\right)\right), \end{aligned} \tag{8}$$

$\overline{\mathrm{GBCS}}$ are the global optimum coordinates, the best solution established as yet, and $\overline{\mathrm{CBCS}}$ is a 2D formation bearing the current finest coordinates of drone.

The two departures are the arrays $\overline{\mathrm{GBCS}}$ and $\overline{\mathrm{CBCS}}$ drone. The design of motion from a fixed leaving point is crucial as this omits shortening of the explored space toward the origin.

4.3. Drone Movement. To reach at target position drones, we utilize an autonomous trick. After reaching the target destination, drones acquire information and then send it to the command centre. Methods obtainable to DSO for computing target location are harvested at different evolutionary and nonevolutionary algorithms. The main aim here is to discover the goal position of every drone in every squad. Conceptually, there are two ways to complete its task. Either refashioning with the finest coordinates established up to now for generating T_mC (a two-dimensional structure containing a team's coordinates) or no recombination conceivably. Definitely, the option is haphazard, but all amalgamation methods accessible to the drones have the equal chance of being selected. At last, the drones get permission to proceed narrowly inmost a predefined perimeter. In such a case, it is necessary to correct T_mC coordinates if they occur outside a boundary (a breach). There are various correlation techniques available that can be used, and there is no bias in the current DSO to favor one over the other.

The objective function has been computed just after the drone proceeds, and their outcome is forwarded to the command centre for taking judgment like upgrading the firmware.

4.4. Firmware Update. In this condition, hyperheuristic deputize if required. For checking out the standard of a team, the command centre utilizes two chunks of information like (1) its position considering target function data's and (2) the degree of out-of-bound coordinates that they produce. If violations are not considered into account, then better outcomes may not be produced by the correlation methods just by chance. But T_mC had, in reality, huge violations. Team quality is computed at each iteration. The command

centre updates w worst firmware by variations of the w best firmware just after firmware update criteria satisfied. No reassimilation of codes was used there, but it is essential that the current variant fulfils the following mentioned rule:

(i) In the tree data configuration, S is the number of nodes and k is the number of teams, where S_{least} and S_{high} are customized parameters. At the time of updating, $S(P_k)$ should be greater than least and $S(P_k)$ greater than high, where S_{least} and S_{high} are customized parameters.

(ii) As for identifying the actual perturbation from the updated one, the upgraded version does not take into account illustrative variations but only syntactic variations.

(iii) Functions cannot collect the same argument for both parameters at the same time.

(iv) The perturbation strategy of (6) must maintain.

4.5. Choice of Succeeding Iteration, Stagnation Recognition, and Discussion. The drones are able to generate similar are mostly similar prey coordinates after utilizing a specific region of landscape. With the help of convergence avoidance methods, drones are able to run away from local optima, but this mechanism is generally not available in evolutionary algorithms. With the help of scaling, observation, and investigation of inertness, the creation of conflicting coordinates allows proceeding to areas long away from the neighbourhood, but it can bring recession for arriving toward utmost results that may also diminish its perfection. The command centre gives privilege to important data after the drone returns back for what they searched in the landscape (i.e., in cost function). They also store the search plan for near future. Stagnation is noticed when the cost function assessment of the present utmost output at a specific index remains unchanged succeeding a precise amount of repetitions. Quite a number of techniques were implemented by DSO for producing a good sampling strategy to look into various regions in search space for upgrading the interpretation to others.

5. DSO-Based MPPT Approach

Drone squadron optimization is a non-nature-motivated evolutionary metaheuristic that mimics the behaviour of drones that are commanded by a command centre and fly over a region to explore. The duty cycle (D) is treated as an optimistic variable for soft computing optimization problems as a converter is associated with the PV module and MPP may be sleighed by regulating the concerned duty cycle. All the particles meet to the utmost value within very short iterations (i.e., 2-3 iterations) and maximum power we received from the PV module.

Drones, like the man-made undersea machines or the well-known flying vehicles like balloons, aeroplanes, helicopters, and quad-copters, have sensors, can communicate over long distances, and can manoeuvre independently or remotely.

It is important to note that solar energy has the capability to be improved or upgraded not only in terms of physical hardware but also in terms of its software (firmware). As a result, researchers have the opportunity to incorporate mechanisms into the algorithm as common software updates since the artificially constructed machine has a programming program (firmware) that governs its behavior, which is easier than searching for a natural phenomenon to justify the change. A comparison between MPPT and the cuckoo search algorithm (CUSA) [42–45], a comparison between MPPT and particle swarm optimization (PSO), and a comparison between MPPT and grey wolf optimization are presented in order to demonstrate its viability under PSCS. Figure 6 displays the P-V curve and I-V curve for the different irradiance circumstances used in the investigation. In order to analyse the P-V and I-V natures, three shading structures, PSCS 1, PSCS 2, and PSCS 3, are used. Table 1 displays the comparable MPP for each of the PSCS circumstances taken into consideration. Table 2 compares the effectiveness of DSO-based MPPT with other MPPT in terms of maximum overshoot, tracking speed, steady state error, and accuracy. Especially in PSCS 2 and PSCS 3, power tracking by the proposed method is noticeably high compared to others. The flowchart of DSO-based MPPT has been shown in Figure 7.

Table 3 provides a performance comparison analysis of the DSO with GWO and PSO for benchmark function named Langerman-5. In this case study, the objective function, or minimization issue, is taken into consideration in order to obtain the benchmark functions' comparative statistical search performance outcomes over a 100-iteration period. Table 3 shows that the DSO algorithm produced results that were superior to PSO in terms of mean, standard deviation (SD), and best value ($f_{\min}$).

The curve in Figure 8 represents the convergence characteristic for benchmark functions: Langerman-5. Compared to PSO and GWO, Figure 8 demonstrates that the DSO algorithm requires less iterations to reach its global minimal solution.

6. Simulation Results and Outcomes

Simulations performed in MATLAB/SIMULINK software and the performance of DSO-based MPPT are investigated. MATLAB 2018 version was employed to investigate the superior performance of DSO-based MPPT in tracking of GMPP under both normal as well as partial shading conditions. Later, a comprehensive comparison has been made among DSO-based MPPT and other three algorithm-based MPPT like PSO, cuckoo search algorithm (CUSA), and grey wolf optimization (GWO). 1Soltech 1STH-250-WH 250 W panels are utilized. The module specs mentioned above are listed in Table 4. Two alternative modes, including standard test conditions and partial shading conditions, were simulated.

The whole photovoltaic arrangement consists of an MPPT controller along with a boost converter connected with resistive load. Parameters of the boost converter are

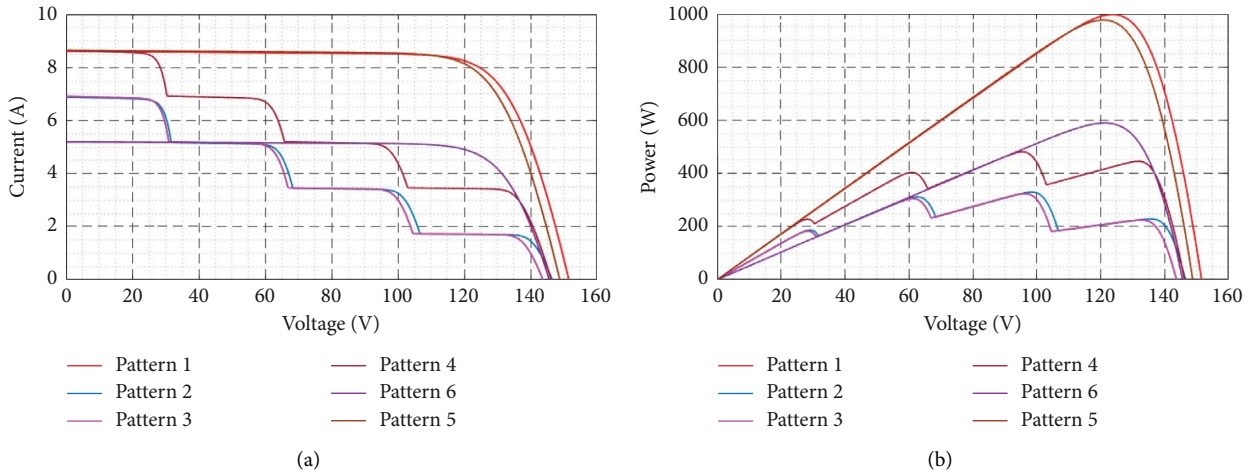

Figure 6: PV panel (a) I-V and (b) P-V characteristics in STC and PSCS conditions.

Table 1: Summarization of irradiances cases used in simulation.

Shading pattern	Types	Module-1	Module-2	Module-3	Module-4
Pattern-1 at 25°C	Uniform shading	1000	1000	1000	1000
Pattern-2 at 25°C	Partial shading	1000	800	600	400
Pattern-3 at 25°C	Partial shading	800	600	400	200
Pattern-4 at 20°C	Uniform shading	1000	1000	1000	1000
Pattern-5 at 20°C	Partial shading	800	600	400	200
Pattern-6 at 50°C	Uniform shading	1000	1000	1000	1000

Table 2: Comprehensive performance analysis with other techniques.

Method	Complexity	Max. overshoot	Performance	Tracking speed	Accuracy	Steady state error
CUSA	Low	Low	Average	Average	Average	Average
PSO	Low	Low	Average	Average	Average	Average
GWO	Low	Average	Average	Average	High	Average
DSO	High	Low	Very good	Excellent	Very high	Less

stated as $C_{IN} = 100\,\mu F$, $C_{OUT} = 100\,\mu F$, and $L = 3$ mH. The resistive load used here has a value of 30 Ω. The switching frequency is set as 10 KHz.

6.1. Performance under Standard Test Conditions and Variable Atmospheric Conditions while Temperature Remains Fixed. Total four conditions have been created which are examined for the performance of the proposed MPPT method: firstly, simulation was done under uniform irradiance conditions, and in this case, the irradiance level is set to 1000 W/m^2, and total four panels have been used. Later, three different cases have been used as an input parameter of PV panels, and the number of PV panels also varies, whereas climate temperature is fixed at 25°C. The primary estimate for duty cycles is so chosen that is equally disperse within the search space range of duty cycle between 0 and 1. Parameters are used for every algorithm chosen depending upon high MPPT efficiency as stated PSO: $w = 0.1$, $C1 = 1.2$, $C2 = 1.2$., and CUSA: beta = 3/2, k coefficient = 0.8.

The simulation outputs of photovoltaic power and load power of aforesaid algorithms for uniform irradiance conditions are given in Figure 9. Power harvested from DSO, CUSA, GWO, and PSO-based MPPTs is shown in graph for total four cases. There are total two types of case studies done here. Firstly, constant irradiance which is 1000 W/m^2 given as an input parameter to solar photovoltaic panel keeping temperature fixed at 25°C and after that performance under three partial shading cases also. For all the cases, the DSO-based MPPT algorithm established its supremacy under various atmospheric conditions. The corresponding comparison is also shown is Table 5.

In the second case, four PV panels have been used where irradiance is maintained at 580-620-860-790 W/m^2. A comprehensive result has been shown in Figure 10. Here also, the power received from DSO-based MPPT is higher among other three methods. Table 6 discusses four MPPT performances when four PV panels are used.

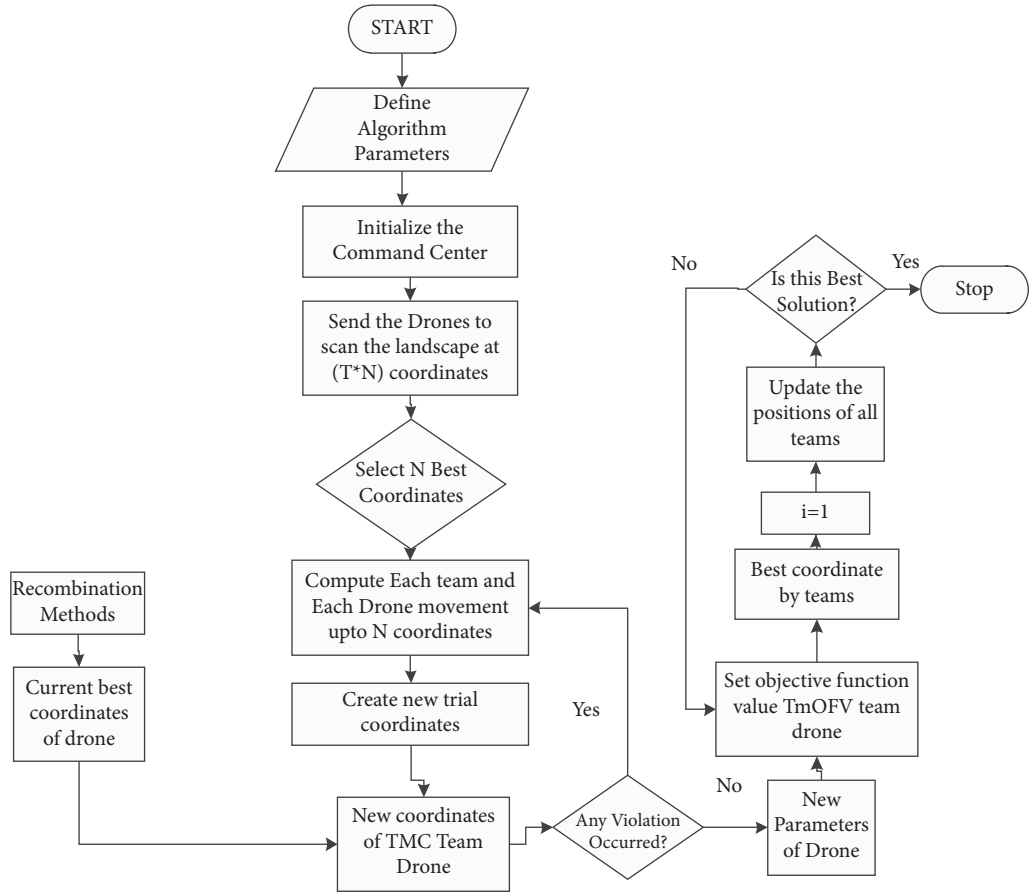

Figure 7: Flow chart of DSO-based MPPT.

Table 3: Comparative performance index of test function: Langerman-5.

Function name	DD	Search space	Statistical value	PSO	GWO	Proposed method (DSO)
Langerman-5	5	[−300, 300]	Best ($f_{\min}$)	4.62×10^{-7}	4.72×10^{-7}	2.74×10^{-7}
			Mean	4.52×10^{-7}	3.69×10^{-7}	2.79×10^{-7}
			SD	0.57×10^{-9}	0.59×10^{-9}	0.52×10^{-9}

Here, DD: number of design variables or dimension, SD: standard deviation, DSO: drone squadron optimization.

In the third case again, four PV panels have been used where irradiance is maintained at 700-800-900-1000 W/m^2. A comparative result has been shown in Figure 11. Again, the power received from DSO-based MPPT is the highest among other three methods. Table 7 discusses four MPPT performances under this special PSCS condition.

Lastly, in the PSCS-3 case again, four PV panels have been utilized, where the irradiance level was kept fixed at [835-725-635-750] W/m^2. Comparison in simulation results has been shown in Figure 12. DSO-based MPPT showed its supremacy here also by drawing maximum power from the PV module. Table 8 discusses four MPPT performances under this PSCS condition.

6.2. Performance under Changes in Temperature. This section has looked at the impact of temperature fluctuation on the operational point of the photovoltaic system, under the assumption that the isolation value is constant at 1000 W/m^2. Temperature is maintained for 25–30-30–35°C, respectively, for four solar panels. Table 9 shows various temperature conditions along with efficiency comparison for different soft computing techniques, while Figure 13 shows PV power and load power comparison with time for various algorithms.

6.3. Performance under Changes in Both Temperature and Irradiance. This section has looked at the impact of temperature fluctuation on the operational point of the photovoltaic system, under the assumption that the irradiance value is also changing at certain intervals of time, taking temperature and irradiance readings every 0.3 seconds. The authors of the case study chose a time range of 0 to 2.0 sec, which denotes irradiance variations at 0.3, 0.6, 0.9, 1.2, 1.5, 1.8, and 2.0 sec. As previously discussed, the corresponding

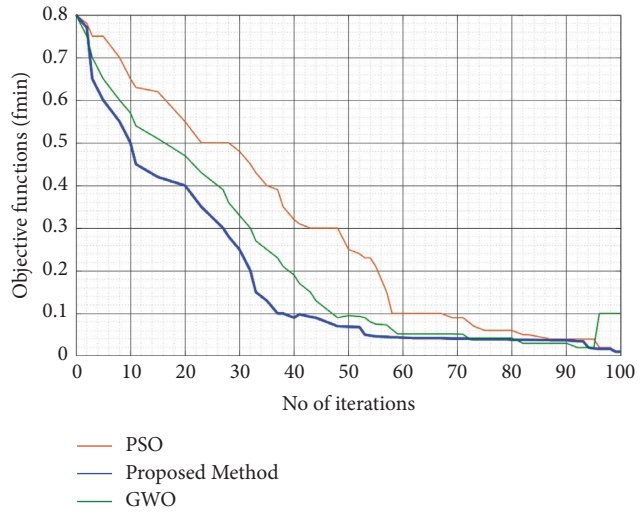

Figure 8: Comparative convergence graph for benchmark function: Langerman-5.

Table 4: Specification of PV module used in simulation.

Specification	Value
Open circuit voltage; V_{oc}	37.30 Volt
Short circuit current; I_{SCN}	8.66 Amp
Coefficient of temperature at V_{OC}	−0.36901 (V/°C)
Coefficient of temperature at I_{sc}	0.086998 (A/°C)
Cells per module (N_{cell})	60
Maximum power	250.205 (W)
Series connected module per string	1
Parallel strings	1

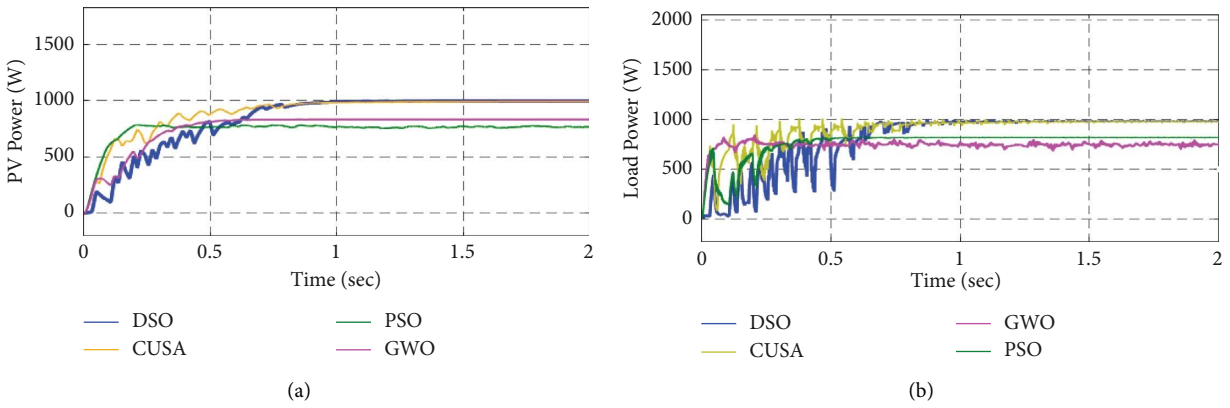

Figure 9: (a) Comparison of PV power; (b) load power in uniform irradiance.

Table 5: Result analysis under uniform irradiance.

Cases	Algorithm	Power at GMPP (W)	Power received (W)	Settling time (sec)	Efficiency
Uniform irradiance (1000 W/m^2)	DSO	998.1	998.0	0.81	99.98
	CUSA		995.4	0.98	99.72
	GWO		769.1	1.11	77.05
	PSO		833.9	0.92	83.54

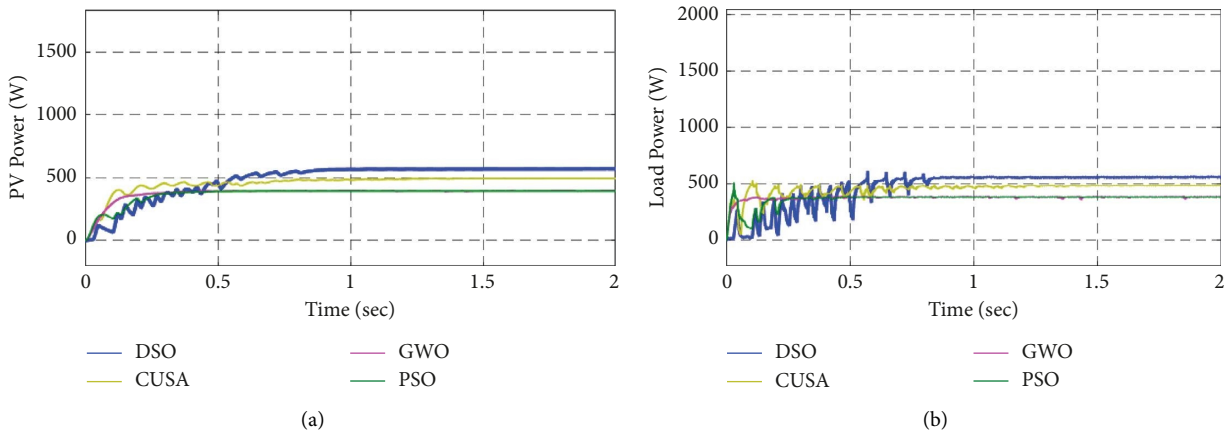

Figure 10: (a) PV power; (b) load power comparison for PSCS-1.

Table 6: Result analysis under PSCS-1.

Case	Algorithm	Power at GMPP (W)	Power received (W)	Settling time (sec)	Efficiency (%)
PSCS-1 irradiance (580-620-860-790 W/m^2)	DSO	627.12	570	0.80	90.90
	CUSA		495.2	0.92	78.96
	GWO		396.2	1.05	63.18
	PSO		394.0	0.83	62.83

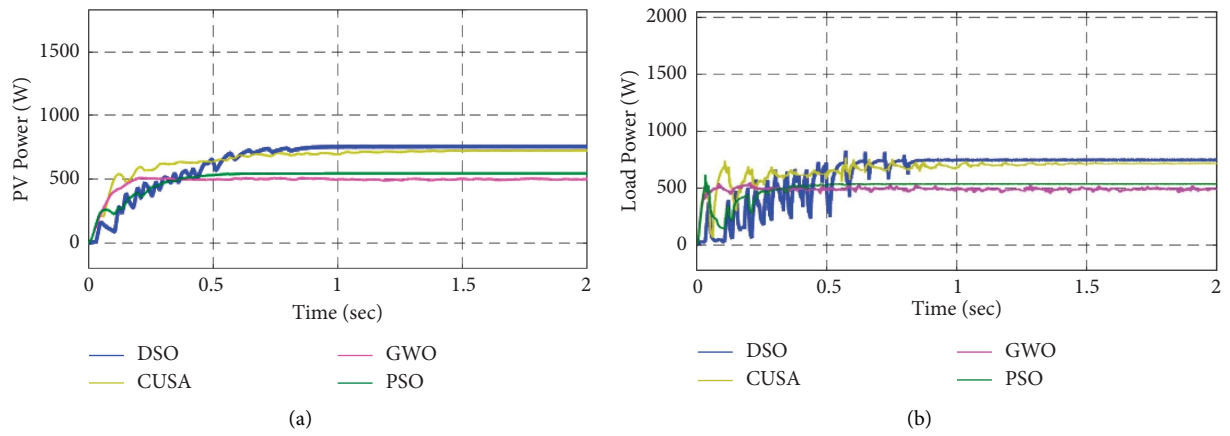

Figure 11: (a) PV power comparison; (b) load power comparison for PSCS-2.

Table 7: Result analysis under PSCS-2.

Case	Algorithm	Power at GMPP (W)	Power received (W)	Settling time (sec)	Efficiency (%)
PSCS-2 irradiance (700-800-900-1000 W/m^2)	DSO	760.77	756.5	0.76	99.43
	CUSA		726.8	0.82	95.53
	GWO		504.0	1.22	66.24
	PSO		546.6	0.80	71.84

temperature changes from 25°C to 40°C every 0.3 seconds, and it then instantly returns to 25°C after 2.0 seconds. Similarly, irradiance values also change at every 0.3 sec interval, starting from 1000 W/m^2 its low down up to 400 W/m^2 at the end of 2.0 sec it settles down at 700 W/m^2. That means this section looks into the dynamic condition of the atmospheric conditions where both solar irradiance as well as temperature are fluctuating. Figure 14(a) depicts the respected PV power output, and 14(b) illustrates a comparative analysis of load power. This figure shows that, in

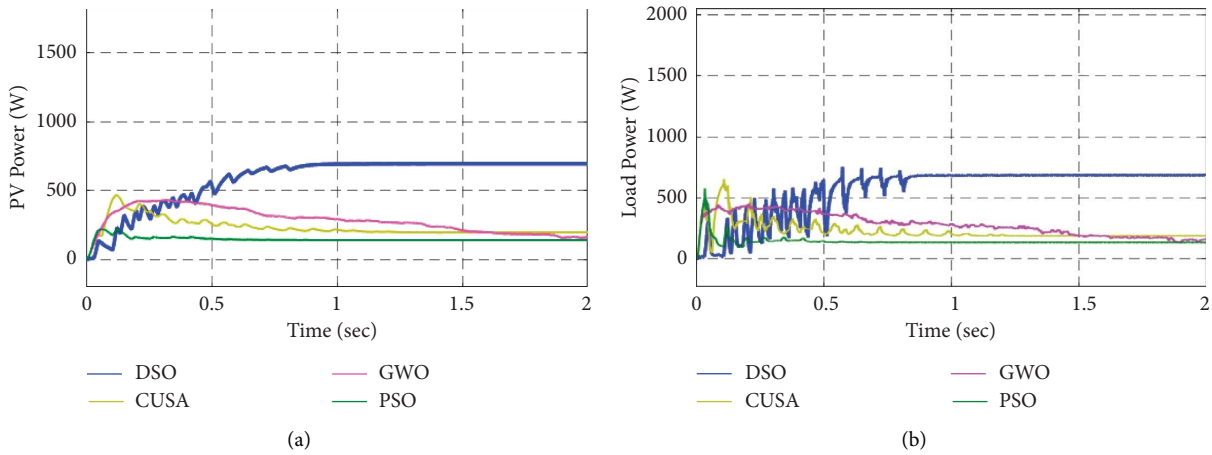

Figure 12: (a) PV power comparison; (b) Load Power comparison for PSCS-3.

Table 8: Result analysis under PSCS-3.

Case	Algorithm	Power at GMPP (W)	Power received (W)	Settling time (sec)	Efficiency (%)
PSCS-3 irradiance (835-725-650-750 W/m^2)	DSO	696.04	695.0	0.62	99.85
	CUSA		194.4	1.45	27.92
	GWO		161.5	1.80	23.02
	PSO		139.6	0.85	20.56

comparison to other techniques, the suggested method employing the drone squadron optimization (DSO) algorithm performs better, is more efficient, has less fluctuation, and has the lowest settling time.

6.4. Performance Evaluation under Presence of Noise and Variation of Load. In this instance, noise and fluctuations in the PV system's load resistance (R) are examined to determine the efficacy and resilience of the suggested DSO algorithm. When voltage and current are measured, as well as when temperature and sun irradiance fluctuations are unpredictable, noise is injected into the system. Figure 15 compares the PV output powers for DSO with PSO and GWO algorithms in the presence of noise/uncertainties and fluctuations in load. Figure 14 shows that compared to PSO and GWO, the DSO-based approach performs better. The technique is still able to achieve the correct MPP in DSO even when the output load is changed. To demonstrate the robustness and dependability of the system, the DSO algorithm is evaluated and compared with PSO, GWO, and CUSA schemes under various PCSs, variations in load, and the existence of uncertainties.

So, in the abovementioned four conditions, where firstly we are fixing the atmospheric temperature and changing the solar irradiance, and secondly, we have changed the temperature while maintaining solar irradiance at 1000 W/m^2 later under dynamic condition both irradiance and atmospheric temperature is changing. Lastly, the performance of DSO-based approach is scrutinized by load variation also. It has been proven from simulation results that the proposed MPPT methods are much superior to other conventional soft computing algorithms in terms of the lowest settling time, adequate amount of PV power, and efficiency consideration.

7. DC Microgrid System Analysis

DC microgrid is an energy booster which consists of nonconventional resources with storage systems [46, 47]. Being regionally operated, this microgrid is able to supply energy to the local grid and may be utilized in standalone demands. Here, in this section, it is shown that the DSO-controlled MPPT system has been interfaced with microgrid. For that, the PV panel used for microgrid connection has specifications which are given in Table 10. DC microgrid topology connected with a solar MPPT controller along with a boost converter is shown in Figure 16.

Partial PV irradiance in these circumstances after every 0.3 sec has been changed in the MATLAB/SIMULINK model, and correspondence PV voltage has been manifested in Figure 17, whereas Figures 18(a) and 18(b) illustrated DC bus voltage and power. Corresponding battery voltage and current graph with time have been displayed in Figures 19(a) and 19(b).

In the proposed system, the battery voltage is consistently maintained at 250 Volts. When the PV voltage exceeds the load voltage, the system facilitates charging of the lithium-ion battery. Conversely, during instances where the PV voltage is not significantly higher than the load voltage, the system ensures the seamless supply of power to the load. The graphical representations in Figures 17 to 19 illustrate a comprehensive comparison between the DSO-based MPPT system integrated with a DC microgrid and alternative algorithms such as CUSA

Table 9: Result analysis under temperature variation.

Case	Algorithm	Power at GMPP (W)	Power received (W)	Settling time (sec)	Efficiency (%)
Irradiance (1000 W/m^2) temperature maintained at 25-30-30-35°C	DSO	977.57	719.6	0.63	73.61
	CUSA		428.5	1.20	43.83
	GWO		373.7	1.64	38.22
	PSO		204.4	0.97	20.90

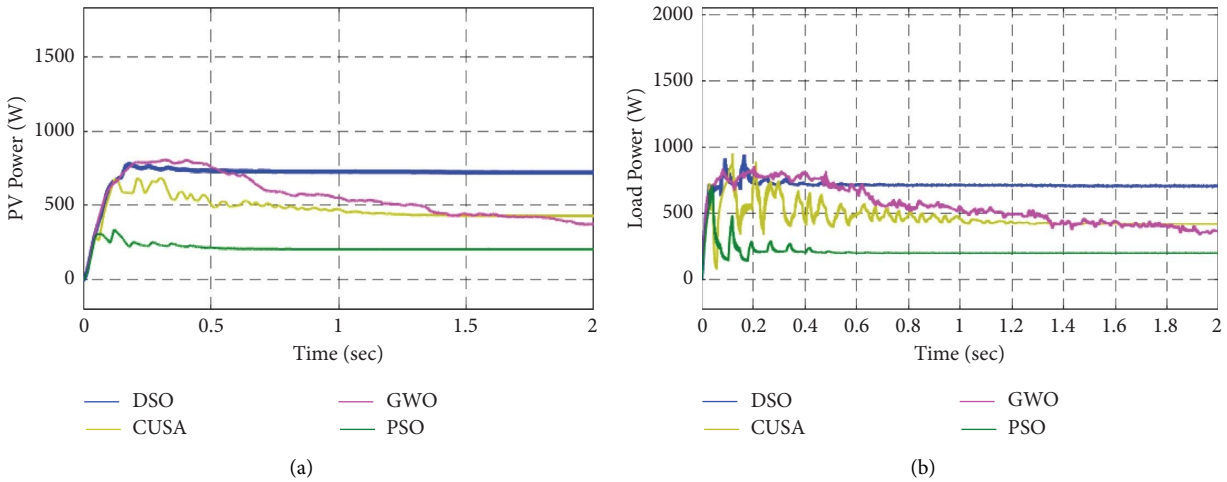

Figure 13: (a) PV power comparison; (b) load power comparison under temperature variation.

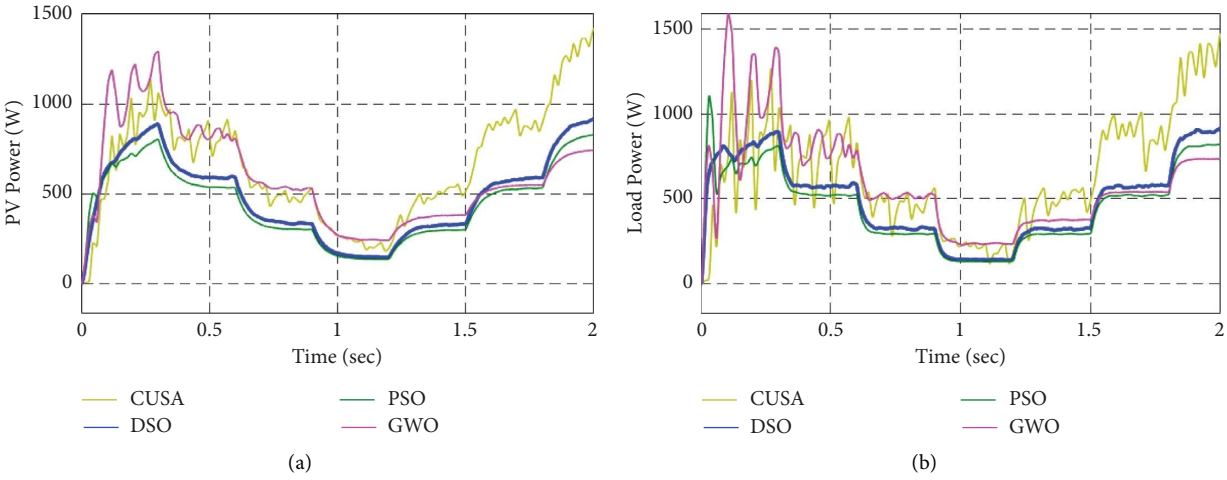

Figure 14: (a) PV power comparison; (b) load power comparison in dynamic condition.

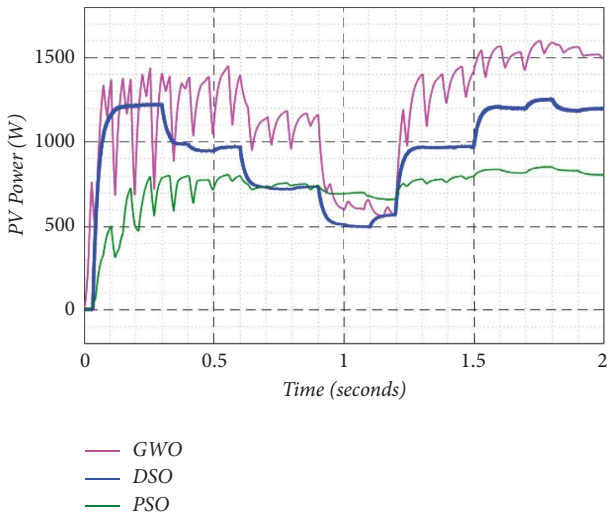

Figure 15: Comparative analysis of dynamic response of PV power.

Table 10: Specifications of the PV module used in simulation with microgrid interfacing.

Specification	Value
Open circuit voltage (V_{oc})	37.30 (V)
Short circuit current (I_{SCN})	8.66 (A)
Coefficient of temperature at (V_{OC})	−0.36901 (V/°C)
Coefficient of temperature at (I_{sc})	0.086991 (A/°C)
Cells per module (N_{cell})	60
Maximum power	250.205 (W)
Series connected module per string	8
Parallel strings	1

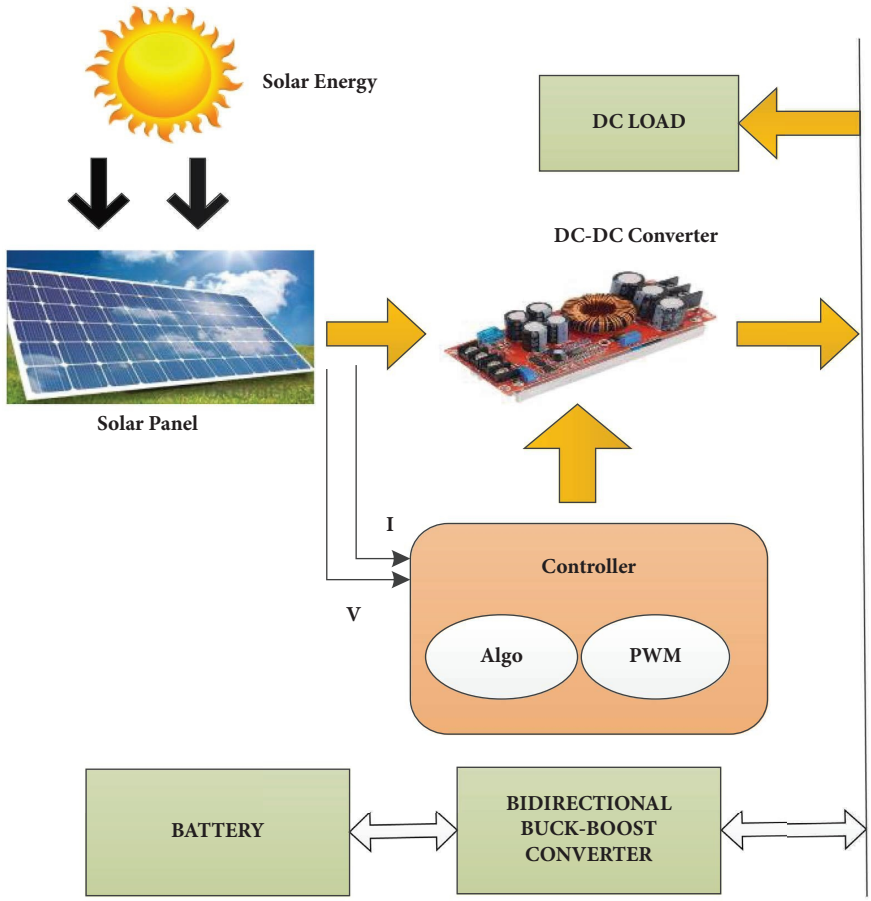

Figure 16: DC microgrid topology with the solar MPPT system.

and flying squirrel search algorithm. Figure 17 shows the PV voltage comparison of the proposed MPPT technique with two well-known and established soft computing-based MPPT algorithms, i.e., cuckoo search algorithm (CUSA) and flying squirrel search algorithm (FSSO). It is worthwhile to say that newly developed MPPT algorithms are much more stable even in partial shading conditions also in contrast with the other two techniques. The DC bus voltage comparison among the three techniques is clearly shown in Figure 18(a) whether Figure 18(b) represents PV power comparison while being connected with DC microgrid. Power oscillation in CUSA and FSSO-based techniques is quite larger whether the proposed drone squadron-based MPPT controller contrasted with DC microgrid gives much lesser power oscillation. In Figure 19(a), battery voltage has been represented. A stable and constant voltage can be seen here in this figure. The battery current of the DSO-based technique with the other two metaheuristic algorithms is well shown in Figure 19(b). A discernible observation indicates that the DSO-based MPPT system, when connected to a DC microgrid, demonstrates superior capabilities in harvesting stable power, current, and voltages compared to other soft computing-based algorithms.

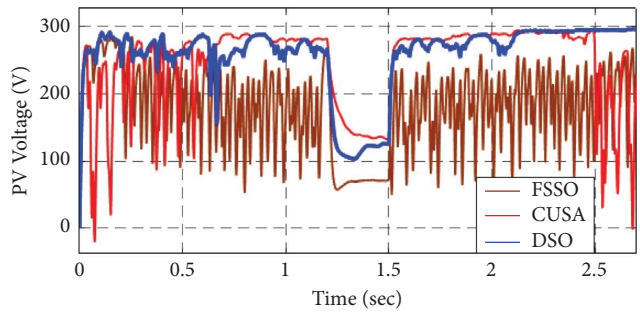

Figure 17: PV voltage with grid connection.

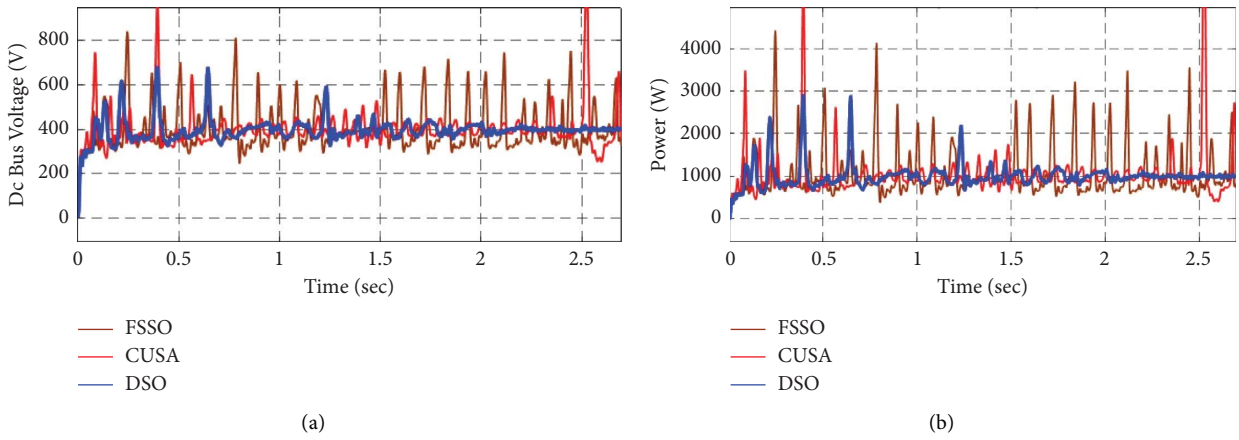

Figure 18: (a) DC bus voltage and (b) power.

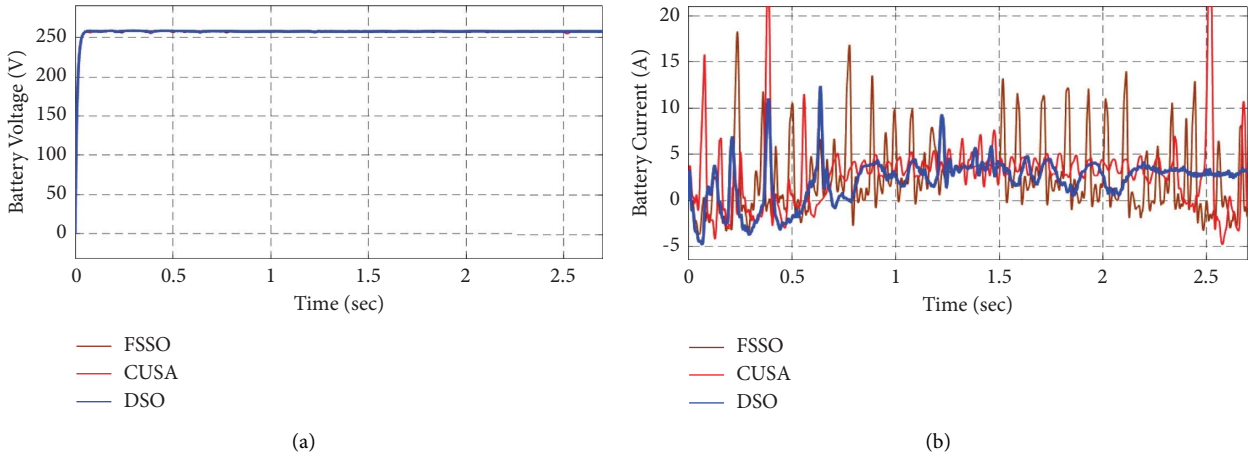

Figure 19: (a) Battery voltage and (b) current graph with time.

8. Conclusion

This work presents a novel maximum power point tracking (MPPT) technique that has the advantages of less setup time, less computing overhead, and less system knowledge requirements. The simulation results are compared with those of three widely used algorithms, PSO, GWO, and CUSA, which are well known in the literature. The effectiveness of the proposed method is validated as well as its performance under various partial shading scenarios. Performance measures include the time it takes to reach the maximum power point (MPP) and the corresponding output power under various partial shading scenarios. After a comprehensive analysis of the data, it is concluded that the suggested method routinely beats current methods in both partial and uniform shading circumstances. Performance measures include the time it takes to reach the maximum power point (MPP) and the corresponding output power under various partial shading scenarios. Increased efficiency, dependability, and sustainability in solar photovoltaic PV

systems are achieved through the integration of the recently created drone squadron algorithm with a DC microgrid platform. This methodology is validated using MATLAB/SIMULINK, and the results show that it performs better than conventional MPPT methods.

In addition to showing a noticeable improvement, the DSO-based MPPT has a bidirectional power flow control technique that can be adjusted to different weather situations. This study also highlights the possibility of a PV-based energy storage system incorporated into a small-scale DC microgrid, which might lead to the production and distribution of power in a more sustainable manner in the future. The next stage of this research is to create a microgrid that is solar-powered and intended to charge electric vehicles. The increasing number of electric vehicles on the road highlights how crucial it is to handle EV charging issues in the context of a microgrid, furthering the shift toward a more sustainable energy environment. There is a great deal of space for this research to be expanded upon in the future [48, 49].

(a) Real-time analysis with hardware configuration of the DSO-based MPPT method is the prime concern of the authors.

(b) Integration of the developed MPPT method with three phase grids.

Nomenclature

ABC: Artificial bee colony
ACO: Ant colony optimization
BC: Boost converter
CUSA: Cuckoo search algorithm
DSO: Drone squadron optimization
FLCR: Fuzzy logic controller
FPA: Flower pollination algorithm
FSSO: Flying squirrel search algorithm
GA: Genetic algorithm
GHO: Grasshopper optimization
GMPP: Global maximum power point
GWO: Grey wolf optimization
HCA: Hill-climbing algorithm
LMPP: Local maximum power point
MPPT: Maximum power point tracking
NNK: Neural network
PSCS: Partial shading condition
PSO: Particle swarm optimization
PV: Photovoltaic
P&O: Perturb and observation
RERS: Renewable energy resources
SSO: Slap swarm optimization
STC: Standard test conditions
TLBO: Teaching-learning-based optimization.

Data Availability

No data were used to support the findings of this study.

Conflicts of Interest

The authors declare that they have no conflicts of interest.

Acknowledgments

Open access funding was provided by the Qatar National Library.

References

[1] M. Kumar, K. P. Panda, J. C. Rosas-Caro, A. V. Gonzalez, and G. Panda, "Comprehensive review of conventional and emerging maximum power point tracking algorithms for uniformly and partially shaded solar photovoltaic systems," *IEEE Access*, vol. 11, pp. 31778–31812, 2023.

[2] A. Ali, K. Almutairi, S. K. Padmanaban et al., "Investigation of MPPT techniques under uniform and non-uniform solar irradiation condition–A retrospection," *IEEE Access*, vol. 8, pp. 127368–127392, 2020.

[3] D. Venkatramanan and V. John, "Dynamic modeling and analysis of buck converter based solar PV charge controller for improved MPPT performance," *IEEE Transactions on Industry Applications*, vol. 55, no. 6, pp. 6234–6246, 2019.

[4] D. S. Pillai and N. Rajasekar, "An MPPT based sensorless line-line and line-ground fault detection technique for PV systems," *IEEE Transactions on Power Electronics*, vol. 34, no. 9, pp. 8646–8659, 2019.

[5] K. Y. Yap, C. R. Sarimuthu, and J. M. Y. Lim, "Artificial intelligence based MPPT techniques for solar PV systems: a review," *IEEE Transactions on Power Electronics*, vol. 8, no. 6, pp. 1043–1059, 2020.

[6] M. Dhimish, "Assessing MPPT techniques on hot-spotted and partially shaded photovoltaic modules:comprehensive review based on experimental data," *IEEE Transactions on Electron Devices*, vol. 66, no. 3, pp. 1132–1144, 2019.

[7] M. A. Elgendy, B. Zahawi, and D. J. Atkinson, "Assessment of perturb and observe MPPT algorithm implementation techniques for PV pumping applications," *IEEE Transactions on Sustainable Energy*, vol. 3, no. 1, pp. 21–33, 2012.

[8] M. Lasheen and M. Abdel-Salam, "Maximum power point tracking using Hill Climbing and ANFIS techniques for PV applications: a review and a novel hybrid approach," *Energy Conversion and Management*, vol. 171, pp. 1002–1019, 2018.

[9] M. Lasheen, A. K. Abdel Rahman, M. Abdel-Salam, and S. Ookawara, "Adaptive reference voltage based MPPT technique for PV applications," *IET Renewable Power Generation*, vol. 11, no. 5, pp. 715–722, 2017.

[10] Y. Cui, Z. Yi, J. Duan, D. Shi, and Z. wang, "A rprop-neural-network-based PV maximum power point tracking algorithm with short-circuit current limitation," in *Proceedings of the IEEE Power and Energy Society Innovative Smart Grid Technologies Conference*, Piscataway, NJ, USA, June 2019.

[11] J. Prasanth Ram and N. Rajasekar, "A novel flower pollination based global maximum power point method for solar maximum power point tracking," *IEEE Transactions on Power Electronics*, vol. 32, no. 11, pp. 8486–8499, 2017.

[12] K. S. Tey, S. Mekhilef, M. Seyedmahmoudian, B. Horan, A. T. Oo, and A. Stojcevski, "Improved differential evolution-based MPPT algorithm using SEPIC for PV systems under partial shading conditions and load variation," *IEEE Transactions on Industrial Informatics*, vol. 14, no. 10, pp. 4322–4333, 2018.

[13] D. S. Pillai, J. P. Ram, A. M. Y. M. Ghias, M. A. Mahmud, and N. Rajasekar, "An Accurate,Shade detection-based hybrid maximum power point tracking approach for PV systems," *IEEE Transactions on Power Electronics*, vol. 35, no. 6, pp. 6594–6608, 2020.

[14] R. Anand, D. Swaroop, and B. Kumar, "Global maximum power point tracking for PV array under partial shading using cuckoo search," in *Proceedings of the IEEE 9th Power India International Conference (PIICON)*, Delhi, India, June 2020.

[15] C. Yanarates, Y. Wang, and Z. Zhou, "Unity proportional gain resonant and gain scheduled proportional (PR-P) controller-based variable perturbation size real-time adaptive perturb and observe (P&O) MPPT algorithm for PV systems," *IEEE Access*, vol. 9, 2021.

[16] M. Bouksaim, M. Mekhfioui, and M. N. Srifi, "Design and implementation of modified INC, conventional INC, and fuzzy logic controllers applied to a PV system under variable weather conditions," *Design*, vol. 5, no. 4, p. 71, 2021.

[17] H. D. Tafti, A. Sangwongwanich, Y. Yang, J. Pou, G. Konstantinou, and F. Blaabjerg, "An adaptive control scheme for flexible power point tracking in photovoltaic systems," *IEEE Transactions on Power Electronics*, vol. 34, no. 6, pp. 5451–5463, 2019.

[18] K. Loukil, H. Abbes, H. Abid, M. Abid, and A. Toumi, "Design and implementation of reconfigurable MPPT fuzzy controller for photovoltaic systems," *Ain Shams Engineering Journal*, vol. 11, no. 2, pp. 319–328, 2020.

[19] S. K. Padmanaban, C. Dhanamjayulu, and B. Khan, "Artificial neural network and Newton raphson (ANN-NR) algorithm based selective harmonic elimination in cascaded multilevel inverter for PV applications," *IEEE Access*, vol. 9, pp. 75058–75070, 2021.

[20] N. Priyadarshi, S. K. Padmanaban, J. B. Holm-Nielsen, F. Blaabjerg, and M. S. Bhaskar, "An experimental estimation of hybrid ANFIS–PSO-based MPPT for PV grid integration under fluctuating sun irradiance," *IEEE Systems Journal*, vol. 14, no. 1, pp. 1218–1229, 2020.

[21] K. L. Lian, J. H. Jhang, and I. S. Tian, "A maximum power point tracking method based on perturb-and-observe combined with particle swarm optimization," *IEEE Journal of Photovoltaics*, vol. 4, no. 2, pp. 626–633, 2014.

[22] K. Sundareswaran, V. Vigneshkumar, and S. Palani, "Development of a hybrid genetic algorithm/perturb and observe algorithm for maximum power point tracking in photovoltaic systems under non-uniform insolation," *IET Renewable Power Generation*, vol. 9, no. 7, pp. 757–765, 2015.

[23] S. Mohanty, B. Subudhi, and P. K. Ray, "A Grey wolf-assisted perturb & observe MPPT algorithm for a PV system," *IEEE Transactions on Energy Conversion*, vol. 32, no. 1, pp. 340–347, 2017.

[24] U. Chauhan, H. Chhabra, A. Rani, B. Kumar, and V. Singh, "Efficient MPPT controller for solar PV system using GWO-CS optimized fuzzy logic control and conventional incremental conductance technique," *Iran J Sci Technol Trans Electr Eng*, vol. 47, no. 2, pp. 463–472, 2023.

[25] K. Sundareswaran, V. Vigneshkumar, P. Sankar, S. P. Simon, P. Srinivasa Rao Nayak, and S. Palani, "Development of an improved P& O algorithm assisted through a Colony of foraging ants for MPPT in PV system," *IEEE Transactions on Industrial Informatics*, vol. 12, no. 1, pp. 187–200, 2016.

[26] S. Padmanaban, N. Priyadarshi, M. Sagar Bhaskar, J. B. Holm-Nielsen, V. K. Ramachandaramurthy, and E. Hossain, "A hybrid ANFIS-ABC based MPPT controller for PV system with anti-islanding grid protection: experimental realization," *IEEE Access*, vol. 7, pp. 103377–103389, 2019.

[27] A. F. Mirza, M. Mansoor, Q. Ling, B. Yin, and M. Y. Javed, "A salp-swarm optimization based mppt technique for harvesting maximum energy from PV systems under partial shading conditions," *Energy Conversion and Management*, vol. 209, Article ID 112625, 2020.

[28] B. Yang, L. Zhong, X. Zhang et al., "Novel bio-inspired memetic salp swarm algorithm and application to mppt for pv systems considering partial shading condition," *Journal of Cleaner Production*, vol. 215, pp. 1203–1222, 2019.

[29] M. Mansoor, A. F. Mirza, Q. Ling, and M. Y. Javed, "Novel grass hopper optimization based mppt of pv systems for complex partial shading conditions," *Solar Energy*, vol. 198, pp. 499–518, 2020.

[30] A. H. Elmetwaly, R. A. Younis, A. A. Abdelsalam et al., "Modeling, simulation, and experimental validation of a novel MPPT for hybrid renewable sources integrated with UPQC: an application of jellyfish search optimizer," *Sustainability*, vol. 15, no. 6, p. 5209, 2023.

[31] C. Manickam, G. R. Raman, G. P. Raman, S. I. Ganesan, and C. Nagamani, "A hybrid algorithm for tracking of GMPP based on P&O and PSO with reduced power oscillation in string inverters," *IEEE Transactions on Industrial Electronics*, vol. 63, no. 10, pp. 6097–6106, 2016.

[32] N. F. Ibrahim, M. M. Mahmoud, A. M. H. A. Thaiban et al., "Operation of grid-connected PV system with ANN-based MPPT and an optimized LCL filter using GRG algorithm for enhanced power quality," *IEEE Access*, vol. 11, pp. 106859–106876, 2023.

[33] C. Pradhan, M. K. Senapati, S. G. Malla, P. K. Nayak, and T. Gjengedal, "Coordinated power management and control of standalone PV-hybrid system with modified IWO-based MPPT," *IEEE Systems Journal*, vol. 15, no. 3, pp. 3585–3596, 2021.

[34] D. A. Nugraha, K. L. Lian, and Suwarno, "A novel MPPT method based on cuckoo search algorithm and golden section search algorithm for partially shaded PV system," *Canadian Journal of Electrical and Computer Engineering*, vol. 42, no. 3, pp. 173–182, 2019.

[35] S. A. Gorji, H. G. Sahebi, M. Ektesabi, and A. B. Rad, "Topologies and control schemes of bidirectional DC–DC power converters: an overview," *IEEE Access*, vol. 7, pp. 117997–118019, 2019.

[36] Y. Li, Z. Tang, Z. Zhu, and Y. Yang, "A novel MPPT circuit with 99.1% tracking accuracy for energy harvesting," *Analog Integrated Circuits and Signal Processing*, vol. 94, no. 1, pp. 105–115, 2018.

[37] W. I. Hameed, A. L. Saleh, B. A. Sawadi, Y. I. A. Al-Yasir, and R. A. Abd-Alhameed, "Maximum power point tracking for photovoltaic system by using fuzzy neural network," *Inventions*, vol. 4, no. 3, p. 33, 2019.

[38] C. Pradhan, M. K. Senapati, N. K. Ntiakoh, and R. K. Calay, "Roach infestation optimization MPPT algorithm for solar photovoltaic system," *Electronics*, vol. 11, no. 6, p. 927, 2022.

[39] V. V. de Melo and W. Banzhaf, "Drone squadron optimization: a self-adaptive algorithm for global numerical optimization," *Neural Comput & Applic, the Natural Computing Applications Forum*, vol. 56, 2017.

[40] F. Peng, K. Tang, G. Chen, and X. Yao, "Population-based algorithm portfolios for numerical optimization," *IEEE Transactions on Evolutionary Computation*, vol. 14, no. 5, pp. 782–800, 2010.

[41] S. Jana, P. K. Biswas, and C. Sain, "Mathematical modeling of impulse island controller to safely store the energy from high-voltage lightning impulse," *Energy Storage*, vol. 4, no. 4, 2022.

[42] A. Roy, A. Ghosh, C. Sain, F. Ahmad, and L. Al-Fagih, "A comprehensive analysis of control strategies for enhancing

regulation in standalone photovoltaic systems," *Energy Reports*, vol. 10, pp. 4659–4678, 2023.

[43] T. Barker, A. Ghosh, C. Sain, F. Ahmad, and L. Al-Fagih, "Efficient ANFIS-driven power extraction and control strategies for PV-bess integrated electric vehicle charging station," *Renewable Energy Focus*, vol. 48, pp. 100523–100617, 2024.

[44] A. Ganguly, P. K. Biswas, S. Chiranjit, T. A. Ahmad, R. M. Ahmed, and S. Ahmed, "Horse herd optimized intelligent controller for sustainable PV interface grid-connected system: a qualitative approach," *Sustainability*, vol. 15, no. 14, pp. 1–26, 2023.

[45] R. Anand, D. Swaroop, and B. Kumar, "Global maximum power point tracking for PV array under partial shading using cuckoo search," in *Proceedings of the 2020 IEEE 9th Power India International Conference (PIICON)*, pp. 1–6, Sonepat, India, July 2020.

[46] M. K. Senapati, C. Pradhan, S. R. Samantaray, and P. K. Nayak, "Improved power management control strategy for renewable energy-based DC micro-grid with energy storage integration," *IET Generation, Transmission & Distribution*, vol. 13, no. 6, pp. 838–849, 2019.

[47] M. K. Senapati, C. Pradhan, and R. K. Calay, "A computational intelligence based maximum power point tracking for photovoltaic power generation system with small-signal analysis," *Optimal Control Applications and Methods*, vol. 44, no. 2, pp. 617–636, 2021.

[48] A. Sagonda, K. Folly, and P. Kenneth Ainah, "Comparison of three techniques for maximum power point tracking of solar PV," in *Proceedings of the IEEE Intentional Conference on Fuzzy Systems*, Napoli, Italy, August 2018.

[49] A. Ganguly, P. K. Biswas, C. Sain, and T. S. Ustun, "Modern DC–DC power converter topologies and hybrid control strategies for maximum power output in sustainable nanogrids and picogrids-A comprehensive survey," *Technologies*, vol. 11, no. 4, p. 102, 2023.